



City Research Online

City, University of London Institutional Repository

Citation: Mitolidis, G. J., Salonikios, T. N. & Kappos, A. J. (2012). Tests on RC Beams Strengthened at the Span with Externally Bonded Polymers Reinforced with Carbon or Steel Fibers. *Journal of Composites for Construction*, 16(5), pp. 551-562. doi: 10.1061/(asce)cc.1943-5614.0000281

This is the accepted version of the paper.

This version of the publication may differ from the final published version.

Permanent repository link: <https://openaccess.city.ac.uk/id/eprint/13903/>

Link to published version: [https://doi.org/10.1061/\(asce\)cc.1943-5614.0000281](https://doi.org/10.1061/(asce)cc.1943-5614.0000281)

Copyright: City Research Online aims to make research outputs of City, University of London available to a wider audience. Copyright and Moral Rights remain with the author(s) and/or copyright holders. URLs from City Research Online may be freely distributed and linked to.

Reuse: Copies of full items can be used for personal research or study, educational, or not-for-profit purposes without prior permission or charge. Provided that the authors, title and full bibliographic details are credited, a hyperlink and/or URL is given for the original metadata page and the content is not changed in any way.

City Research Online:

<http://openaccess.city.ac.uk/>

publications@city.ac.uk

1 Tests on R/C Beams Strengthened at the Span with Externally-bonded Polymers, 2 Reinforced with Carbon or Steel Fibers

3 George J. Mitoilidis¹, Thomas N. Salonikios², Andreas J. Kappos³

4 Abstract

5 The main objective of the experimental work reported herein is the comparative evaluation of Steel-
6 Reinforced (SRP) and Carbon- Reinforced (CFRP) Polymers used as externally-bonded reinforcement
7 in strengthening of reinforced concrete (R/C) members. Tensile stress-strain, as well as bond
8 constitutive laws for these materials were first derived from sixteen tests and are summarized here.
9 Results are then reported from four-point bending tests of five full-scale R/C beams strengthened at
10 their span using SRP and CFRP strips. The bond tests have shown that by providing a bond length
11 greater than the effective one, neither the bond strength nor the deformation capacity are increased,
12 whereas by increasing the width of the strip the bond strength is increased. From the bending tests of
13 beams it was found that the use of both SRP and CFRP strips resulted in a significant increase in
14 strength (up to 92%) with respect to the strength of the initial specimen. The experimentally measured
15 strengths were estimated analytically, using both the experimental measurements of the specimen
16 deformations and the pertinent provisions of ACI 440 and Eurocode 8-Part 3.

17 **Keywords:** SRP; CFRP; R/C beams; flexural strengthening; testing

19 Introduction

20 The use of carbon fiber-reinforced polymers (CFRP) for strengthening R/C beams has been the subject
21 of several investigations in the last decades, and the efficiency of this material in increasing the
22 flexural strength of beams has been shown. During the last decade, research has also focused on
23 strengthening of R/C members using steel-reinforced polymers (SRP). Relevant tests carried out so far
24 addressed the strength of the SRP material (typically in the form of strips), bond with concrete, and
25 means of improving their anchorage conditions.

26 Among the researchers that investigated experimentally the mechanical properties of SRP
27 materials, Kim et al. (2005) tested SRP type 3X2 cords (made by twisting 5 individual wires together)
28 and reported data on their modulus of elasticity, tensile strength, Poisson ratio, and ultimate strain.
29 Huang et al. (2005) studied experimentally the properties of SRP type 12X cords (made by twisting
30 three 0.22 mm wires and nine 0.20 mm wires together) and compared them with theoretical
31 predictions from micromechanics equations, to evaluate the reliability of these equations; they found

¹ Consulting Engineer, former research student, at the Aristotle University of Thessaloniki, Greece

² Researcher, Structural Division, Institute of Engineering Seismology and Earthquake Engineering, Thessaloniki, Greece

³ Professor, Civil Engineering Department, Aristotle University of Thessaloniki, 54124 Thessaloniki, Greece

1 that the mechanical properties of SRP cords can be predicted with reasonable accuracy with the aid of
2 micromechanics models. Barton et al. (2005) tested dog bone shaped strips, consisting of 3X2 cords
3 embedded either in polymeric resin (SRP) or in cementitious grout (SRG). It was found that SRP's
4 have a higher modulus of elasticity and shear modulus than SRG's.

5 Among the researchers that studied bond between SRP (and/or SRG) and concrete surfaces,
6 Matana et al (2005), conducted direct shear tests on specimens including 3X2 and 3SX cords (three
7 identical wires twisted together at a longer than usual lay length and then over-wrapped with a single
8 wire) embedded in polymeric resin or cementitious grout. It was found that SRP strips separated from
9 the concrete substrate attracting the outer surface of concrete, while in SRG specimens debonding
10 occurred at the interface between the SRG strip and the concrete surface. The required bond length for
11 SRG was found to be almost double that for SRP. Figeys et al. (2005) studied the bond mechanism
12 between SRP and concrete by means of direct tension tests. Test results were compared with
13 predictions of models originally developed for CFRP (the average ratio of experimental/analytical
14 values was 1.16) with predictions of models proposed by the authors (average ratio of 1.02). Cancelli
15 et al. (2007), also studied bond between SRP and SRG, and the concrete substrate. They found that
16 maximum strength, load transfer mechanism, and ultimate failure mode are all influenced by the type
17 of the matrix (polymeric resin or grout). More specifically, in specimens where epoxy resin was used
18 peeling of concrete took place, whereas in specimens with cementitious grout debonding occurred at
19 the interface between SRG and concrete, and bond resistance was lower than for the SRP. Toutanji et
20 al. (2007), studied the effect of the number of FRP layers on bond strength. An increase of 15 to 20%
21 (depending on concrete grade) in bond strength was found when an extra layer was added.

22 Among studies that involved strengthening of R/C beams with externally-bonded polymers those
23 by Wobbe et al. (2004), Prota et al (2004), Kim et al. (2005), Huang et al. (2005), Casadei et al.
24 (2005), Figeys et al. (2005), Lopez et al. (2007), Saber et al. (2008) involved comparative evaluation
25 of the relative efficiency of SRP, SRG and CFRP. These studies also included proposals for improving
26 the anchorage (bond) conditions for the materials used. It was found that externally-bonded SRP and
27 SRG strips constitute an effective means for strengthening R/C members. More specifically, flexural
28 strengthening provided by SRP/SRG was found to be equally effective as that provided by CFRP.
29 Specimens strengthened with SRP or SRG developed a higher deformation capacity than similar
30 CFRP-strengthened specimens, while their failure modes were similar to those of CFRP-strengthened
31 specimens. The most common failure mode was a rather brittle debonding (peeling) of the concrete
32 surface, that initiates at the ends of the anchorage zones. The use of either anchors or U-shaped strips
33 perpendicular to the beam axis, was found to delay debonding of the composite strips, leading to an
34 improved flexural behavior of the strengthened specimen.

35 Lopez et al. (2007), strengthened with SRP's the beams of an actual bridge for both flexure (at the
36 span) and shear (at the supports). The results of their tests indicate that SRP's can be applied for the
37 strengthening of structures, without limitations additional to those that normally apply for FRP's. It

1 was also found that, although the design method prescribed in ACI 440.2R-02 (ACI 2002) does not
2 implicitly apply to SRP's, it can nevertheless be used for the design of structural interventions
3 involving these materials.

4 In the present paper, results are first reported from tests aiming at the determination of the
5 mechanical properties of SRP and CFRP strips, as well as the characteristics of bond between these
6 materials and concrete. Then, the experimental set-up and the results from five tests involving full-
7 scale reinforced concrete (R/C) beams are reported; three of these beams were strengthened with SRP
8 or CFRP strips, with a view to increasing their flexural strength. A detailed description of test results
9 involving the materials used for strengthening can be found in previous papers by Mitolidis et al.
10 (2008 a, b) and they are also summarized in this paper, whenever needed.

11 **Research Significance**

12 While a fair number of experimental studies exists dealing with issues related to strengthening of R/C
13 members with CFRP and (to a lesser extent) SRP materials, a review of the existing literature indicates
14 that there are still some issues that require further research. Hence the present study supplements the
15 existing state-of-the-art mainly in the following respects:

- 16 • Bond tests are carried out using an experimental set-up that is different from those used so far,
17 and addresses in a uniform way CFRP strips, and SRP strips with different types of steel cords
18 (3X2 and 12X); moreover, bond tests are carried out for two different concrete grades.
- 19 • A key objective was to study the effectiveness of SRP strengthening of 'old-type' members,
20 since such members are the ones that typically need strengthening. Hence, the 'prototype'
21 beams were designed according to old code provisions, and are characterized by the use of
22 smooth reinforcing bars, and relatively low-strength concrete. Bending tests reported here
23 involve a total of five full-scale beams, two of them without strengthening (one critical in
24 flexure and one critical in shear) and three nominally identical beams strengthened against
25 flexure using CFRP, SRP-3X2, and SRP-12X.
- 26 • In previous studies on reinforced polymer-strengthened beams the anchorage of the composite
27 materials was done in the usual way i.e. they extended one development length beyond the
28 section wherein they were required for flexural resistance, which means that they terminated in
29 an area that is still in tension; moreover, in these areas shear cracks are often present that
30 adversely affect bond conditions. In some of the beams of the present study, anchorage of
31 composite strips extends further towards the support, reaching areas without tensile stresses but
32 also unaffected (due to test set-up) by the compression resulting from an actual support, hence
33 providing more insight into the factors affecting this critical region of the strengthened
34 members.
- 35

- Another objective was to assess the reliability of international codes/guidelines for strengthening with externally bonded reinforced polymers, which were developed for FRP reinforcement and are not necessarily adequate for SRP strengthening. Hence, in the analytical part of the study the flexural, as well as the shear, strength of the beams are estimated using the two leading international documents, i.e. the ACI 440R-08 Guidelines and Eurocode 8-Part 3, leading to conclusions particularly relevant to design practice.

Tests for the Estimation of the Mechanical Properties of the Fiber-Reinforced Polymers

For the estimation of the flexural and/or shear strength of R/C elements strengthened with externally-bonded FRPs of SRPs the strain capacity of the reinforced polymer is used. In these cases either the fracture, or the debonding, strain is used, while for design purposes a lower value is introduced, typically through an appropriate safety factor. It is recalled here that for these materials the fracture strain is significantly higher than the debonding strain, Mitolidis et al (2008b). In the case of SRP strips with ample width and proper anchorage, and also of strips with coarsely spaced wires, the fracture strain becomes critical as found by simplified calculations using models available in the literature, see Toutanji et al (2007). In view of these considerations, direct tension, as well as bond, tests were carried out for the composite materials used herein. SRP strips were of two types, SRP 3X2-23-12 and SRP 12X-23-12; the difference in the twisted wire cords used in each type were explained in the Introduction, while more details can be found in Mitolidis et al (2008b). The CFRP strips were Sika[®] Carbodur[®] (type S512). On the basis of direct tension tests (see insert of Fig. 1), stress – strain diagrams were derived for the various strips, and are shown in Figure 1 together with the corresponding diagram for ordinary steel reinforcement; again, more details of the test set-up can be found in Mitolidis et al. (2008b).

Also as part of the present experimental program, 16 bond tests were carried out to estimate the strength of reinforced polymer strips bonded through epoxy on concrete. The main parameters explored were the type of fiber-reinforced polymer (CFRP, SRP3X2, SRP12X), the width of the strip (50 mm, 80 mm), its bond (development) length (150 mm, 300 mm), the compressive strength of concrete used for preparing the prisms on which the reinforced polymers were bonded, and the degree of treatment of the outer surface of the concrete prisms (removal of the cement skin). The experimental set-up used (which is different from those used in past studies) is shown in Fig. 2a.

From the above tests, summarized in Fig. 2b, it was found that the debonding strength of the CFRP laminates was (on average) 30% higher than the debonding strength of the corresponding SRP laminates, which is consistent with the higher elasticity modulus of the CFRPs, compared to the SRPs (see Fig. 1). For the two types of SRP and for CFRP used here the moduli of elasticity given by manufacturers were 77900, 67600 and 160000 MPa respectively. In some of the models found in the literature, and summarized in Toutanji et al (2007), debonding strength is related to the square root of

1 the modulus of elasticity of the reinforced polymer. The debonding load was affected, as expected, by
 2 the width of the strips. For SRP laminates with 80 mm width the debonding load was 45% higher than
 3 the debonding load of the SRP laminates with 50 mm width. It is pointed out that both bond lengths
 4 used for the specimens (150 mm and 300 mm) were higher than the effective length in all cases, hence
 5 no noticeable effect of the bond length was observed in the bond tests. On the other hand, a small
 6 increase was observed in the debonding strength of the reinforced polymers when concrete strength
 7 was increased from 20.0 MPa to 36.9 MPa. The tensile strength of the concrete prisms was estimated
 8 to be 2.2 MPa and 3.3 MPa, respectively; however, it is known that the increase in the debonding
 9 strength is not related to the (conventionally derived) tensile strength of concrete but rather to its
 10 surface (skin) tensile strength. In cases where the concrete surface is not properly roughened, as
 11 purposely done in the high-strength concrete prisms of this work, the expected debonding strength
 12 increase is not reached. Results from these tests are summarized in Table 1. The name of each
 13 specimen denotes the reinforced polymer type (first letters), the strip width in *cm* (the first number),
 14 the strip length in *cm* (the second number), and the concrete grade (normal strength “NS” or high
 15 strength “HS”). The thickness of all specimens is almost the same, 1.23 mm for CFRP laminates and
 16 1.20 mm for SRP laminates. For this reason the ratio of the debonding strengths between the
 17 specimens of table 1, is proportional to the square root of their moduli of elasticity. This is valid for
 18 specimens with the same width. The last column of table 1 lists the values of the ratio:

$$19 \quad \frac{\sqrt{E_i}}{\sqrt{E_{SRP12X}}} \cdot \frac{P_{SRP12X}}{P_i}$$

20 where E_i are the moduli of elasticity for SRP12X, SRP3X and CFRP respectively, and P_i the
 21 debonding strengths of SRP12X, SRP3X and CFRP respectively, given separately for each considered
 22 width value.

23 The debonding strengths of the aforementioned specimens were then estimated using the analytical
 24 models of Chen & Teng (2001), Neubauer & Rostasy (1997), Yang et al. (2001), and Yuan & Wu
 25 (1999), all of them reported by Toutanji et al. (2007). The measured debonding strengths were better
 26 predicted by the analytical model of Chen and Teng. The analytical model of Neubauer and Rostasy
 27 overestimated the experimentally measured strengths, while the models of Yang et al. and Yuan & Wu
 28 underestimated them. Comparisons of experimentally measured debonding strengths with the
 29 analytically calculated values predicted from the models of Chen & Teng and Yang et al. are
 30 presented in Figures 3a and 3b. More details on the experimental set-up (Fig. 2a) devised for the tests,
 31 and the direct tension and bond test results are given in Mitolidis et al. (2008a, 2008b).

32

33 **Design and Description of Strengthened Specimens**

34 The part of the experimental work on which this paper focuses included five full-scale R/C beam
 35 specimens. Two of them, intended as reference specimens, did not embody any interventions, while

1 the remaining three were strengthened against flexure with externally-bonded reinforced polymers.
2 Among the unstrengthened beams, one (SVM) was designed as flexure-critical, and the other (SVS) as
3 shear-critical. The other three specimens were strengthened utilizing SRP 3X2, SRP 12X and CFRP
4 laminates.

5 The nomenclature of the specimens is as follows: The first letter denotes that the specimen
6 represents the “Span” (S) of a continuous beam; the entire program included eight more beam
7 specimens, not reported herein, that represent the support region of a continuous beam. The last letter
8 denotes the expected failure mode of the specimen, “S” for shear failure, “M” for bending moment
9 (flexural) failure. The middle letters refer to the intervention scheme (or absence of it), i.e. “V” for
10 virgin (unstrengthened) specimens, “C” for the specimen strengthened in flexure using CFRP, while
11 for the specimens strengthened with SRP the letters in the middle are “S3X2” and “S12X” denoting
12 the type of steel-reinforced polymer used.

13 The three strengthened specimens SCM, SS12XM and SS3X2M were nominally identical (prior to
14 strengthening) to virgin specimen SVM, and were all designed to fail in a flexural mode. Reinforcing
15 scheme and construction details for all specimens are given in Figure 4, and it is recalled here that the
16 reference beams were designed according to prevailing European practices in the 1970’s. As is
17 common in laboratory testing, the specimens were loaded in four-point flexure, unlike beams in real
18 structures which are subjected to distributed loading. To accommodate the constant shear force in the
19 test beam end regions, bent-up bars ($\emptyset 12/25$) were added along the first and the last thirds of the
20 length of the specimens. Smooth bars were used both as longitudinal flexural reinforcement and as
21 shear reinforcement (bent-up bars and stirrups) in the four flexure-dominated specimens; smooth bars
22 were typically used in pre-1970 R/C construction in Europe and elsewhere. In the shear-critical
23 specimen (SVS) ribbed bars were used as longitudinal reinforcement (the main reason for this was the
24 higher strength of these bars, see Fig. 1, which ensured that the flexural strength was well above the
25 shear strength), while smooth bars were used for the stirrups.

26 The 28-day compressive strength of concrete used 3 to 4 decades ago typically had a specified
27 mean value of 22.5 MPa, referring to 200 mm cube specimens. The concrete used for the specimens of
28 this study had a mean cylinder strength value of 22.0 MPa, corresponding to a cube strength of 26.4
29 MPa, and tensile strength 2.4 MPa. It was estimated that the 28-day cube strength of 22.5 MPa
30 increases to about 26.9 MPa after 30 to 40 years; hence the concrete grade used in the tests was
31 representative of the prevailing grade in the 1970’s, as initially envisaged.

32 For the flexural strengthening of the beam specimens, the previously described CFRP and SRP
33 strips were used. The epoxy resin used for bonding the carbon laminates was Sikadur[®] 30, with
34 modulus of elasticity 12.8 GPa and tensile strength 27 to 32 MPa (manufacturer’s specifications). The
35 epoxy resin used for bonding the SRPs was Sikadur[®] 330 with modulus of elasticity 4.8 GPa and
36 tensile strength 30 MPa. The process according to which these materials were applied on the beam

1 specimens was that specified by the manufacturer. Details of the specimens are given in Figure 4 and a
2 close-up at the support of the specimens is given in Figure 5.

4 **Description of Experimental Set-up and Instrumentation**

5 The hydraulic actuator needed for applying the vertical loading (four-point bending) on the beam
6 specimens was mounted on the reaction frame of the Laboratory of Concrete and Masonry Structures
7 of the Aristotle University as shown in Figure 6; a strong steel beam was used to distribute the
8 actuator force into two point loads. Since the evaluation of the behavior of the specimens well into the
9 inelastic range was a key objective of the study, the loading history consisted of a displacement
10 ‘ramp’, applied at a rate of 1mm/min. The control of the loading rate was made by a digital controller,
11 by comparing the measurements of the sensors of the actuator with the load command several times at
12 each loading step.

13 The displacement and deformation of the specimen were measured by eight externally-mounted
14 displacement sensors (LVDTs). The arrangement of the LVDTs used on the specimen and their
15 nomenclature are given in Figure 7. On the basis of the measurements of these instruments and the
16 records of the actuator’s load shell, load – displacement (or deformation) diagrams were drawn.

18 **Description of Specimen Behavior**

19 The cracking patterns of all specimens after completion of the tests are shown in Figures 8a to 8e.

20 **SVM:** This reference specimen failed, as anticipated, in a flexural mode. At an applied load of 50 kN
21 (shear force of 25 kN at each end) the first flexural cracks formed at the bottom of the beam specimen,
22 distributed along the middle 1 m of the specimen. This occurred because this was the length along
23 which the maximum bending moment was applied (cf. Fig. 4). As the imposed displacement was
24 increased, for a shear force of 57 kN and a mid-span deflection of 9 mm, opening of one flexural crack
25 in the middle of the specimen started. At this location the flexural reinforcement consisting of smooth
26 bars developed significant inelastic deformations. Since these bars were smooth, practically all
27 inelastic deformation concentrated in this critical crack, while the other flexural cracks remained
28 hairline throughout the test. The large deformation at the critical crack was accompanied by
29 detachment of steel bars from the surrounding concrete; this loss of local bond prevented the smooth
30 bars from developing their full flexural capacity, as also verified by comparing the measured strength
31 with the theoretical one calculated on the basis of the ultimate stress in the reinforcement. Hence, at
32 the end of the test all inelastic deformation was concentrated in the critical crack region, while shear
33 deformations were negligible and no visible shear cracks were detected. The latter was attributed to
34 the intentional over-design of the beam in shear (as evident from the shear reinforcement shown at the
35 top of Fig. 4).

1 **SVS:** This specimen, which was designed with adequate flexural reinforcement and inadequate
2 stirrups, failed subsequent to the formation of a major shear crack at the left support. Hairline shear
3 cracks appeared at an applied load of 180 kN (shear force 90 kN). These cracks initiated next to the
4 point of the application of the load (see Fig. 8b). By increasing the imposed displacements, shear
5 cracks opened further, until shear failure of the specimen occurred. The maximum shear force resisted
6 by the beam was 131 kN. At the top of the beam, spalling of concrete and kinking of steel bars
7 occurred, attributed to the inadequate transverse reinforcement (sparsely-spaced stirrups).

8 **SS3X2M, SS12XM, SCM:** These specimens, prior to strengthening, were nominally identical to
9 specimen SVM, and were strengthened using SRP and CFRP strips (Fig. 4) with a view to obtaining a
10 response dominated by flexure. The key response parameters studied were the failure mode and the
11 deformation at failure of the specimens strengthened using different techniques. For the specimens
12 strengthened with SRP strips, higher deformation capacity was expected than for specimens
13 strengthened with CFRP strips, due to the higher deformability of the former (Fig. 1).

14 During the tests, the first flexural cracks formed at an imposed displacement of about 5 mm. These
15 cracks were distributed along the middle two meters of the length of the specimens. It is known that
16 the width of such cracks increases from the neutral axis to the tension fiber of the specimen's section.
17 However, in the strengthened beams the width of flexural cracks at the outer face of the section, where
18 the reinforced polymer strip was applied, was very small and the cracks showed no visible opening.
19 This is attributed to the much stiffer nature (much higher modulus of elasticity than concrete) of the
20 composite strips used (see also Fig. 1). As the applied displacement (and load) increased, flexural
21 cracks kept opening, but still remained almost closed at the lower face of the specimen. This flexural
22 crack configuration (i.e. cracks closed at their lower tip), hints to the fact that Bernoulli's principle
23 does not apply in the case of beams strengthened at their span with externally-bonded FRPs or SRPs.
24 This has the repercussion that the tensile force (due to bending) resisted by steel reinforcement
25 (located at the bottom of the beam, very close to the reinforced polymer layers) is lower than the
26 corresponding force in specimen SVM, for the same level of beam displacement. It was also noted that
27 the flexural cracks in the strengthened beams were distributed along a significantly longer length than
28 in the reference specimen. The stiffness of the strengthened specimens decreased when these flexural
29 cracks formed, and further reduction was noted when loss of bond between concrete and the reinforced
30 polymer started; this loss of bond was perceived by characteristic cracking noises. The reduced
31 stiffness remained almost constant up to debonding of the reinforced polymers from the concrete
32 surface. In all three strengthened specimens, the reinforced polymer strips debonded at approximately
33 the same load (about 220 kN). Debonding of the strips initiated at a flexural crack in the middle region
34 of the beam. Right after debonding, the strength of the specimens was reduced to a value lower than
35 the strength of the unstrengthened specimen (117.6 kN), indicating that, apparently due to the different
36 cracking pattern, steel bars did not develop (at that stage) the stress developed in the bars of the

1 unstrengthened beam. By further increasing the applied displacement, the strength of the specimen
2 increased up to a value close to the strength level of the initial specimen, while all inelastic
3 deformation concentrated in the longitudinal (smooth) reinforcement at one main flexural crack. After
4 that point, the response of the specimen was almost identical to the one of the unstrengthened
5 specimen. Finally, in the strengthened specimens no visible shear deformations and shear cracks were
6 detected, as expected due to the high shear strength provided (see top of Fig. 4).

7

8 **Load – Displacement Characteristics of the Specimens**

9 The measured load vs. displacement diagrams for all specimens are given in Figures 9 to 13. The
10 arrangement of the sensors (LVDTs) and their nomenclature are shown in Figure 7 and those plotted
11 in Figures 9 to 13 are summarized below:

12 “Mid-span Deflection” → MD

13 “Horizontal Mid-span Tension-side Displacement” → HMT

14 “Horizontal Right-span Displacement” → HR

15 “Horizontal Mid-span Compression-side Displacement” → HMC

16 “Diagonal Left-side Displacement” → DL

17 From the recorded load – deflection curve for the unstrengthened specimen SVM (Fig. 9) it is seen
18 that it has an inelastic deformation capacity of at least 30 mm (which is 1/100 of its span). As
19 mentioned in the previous section, only one major flexural crack formed at the mid-span of the
20 specimen (Fig. 8a). As will be shown analytically later on, bond of the smooth bars of this beam was
21 destroyed when the elongation of the bars was lower than the value corresponding to the development
22 of the maximum strength of the reinforcement. The gradual deterioration of bond should be the reason
23 why this specimen maintained a practically constant strength for a broad range of applied
24 displacements, from 9 mm to 30 mm, despite the fact that the stress – strain diagram of smooth
25 reinforcement has a rather short yield plateau, as shown in Figure 1.

26 The shear-critical specimen SVS, that failed in diagonal tension, reached a mid-span deflection of
27 22 mm, but with a noticeable drop in strength; it is pointed out that strength begun to deteriorate at
28 about half the previous deflection. Although fracture of two stirrups was observed, the residual
29 strength of this specimen was rather high; this was attributed to the contribution of the arch
30 mechanism (inclined compression with the longitudinal reinforcement acting as a tie) of shear
31 resistance, since the longitudinal reinforcement was well anchored in the length of the specimens
32 beyond the supports (600 mm on the left and 600 mm on the right, see Figs. 4 and 5), hence more
33 effective in contributing to this mechanism. It is worth noting here that no previous work was found in
34 the literature, on shear failure of beams with longitudinal reinforcement anchored well beyond the
35 supports.

1 In all strengthened specimens the reinforced polymer strip bonded at the bottom was detached at
2 almost the same load. This is justified by noting that debonding occurred by detachment of a layer of
3 the outer concrete cover, and concrete strength was the same in all beams. Since the elastic modulus of
4 SRP strips is lower than that of CFRP, a larger elongation (hence a larger curvature) was required at
5 the bottom of the beam to achieve the same contribution to the flexural resistance. As a result, for
6 specimens strengthened with SRP the strip was found to detach at a displacement 15% higher than that
7 in the specimen strengthened with a CFRP strip.

8 From the recorded force vs. horizontal elongation diagrams at the tension (bottom) side of the
9 central one meter of the beams (HMT), Fig. 10, the most noticeable, yet anticipated, difference is that
10 between the two unstrengthened specimens; in the flexure-dominated SVM significant elongation of
11 the flexural reinforcement took place for a practically constant force, whereas in the shear-dominated
12 specimen SVS after peak strength was reached, elongation not only stopped but also tended to
13 decrease, implying that for this specimen inelastic deformations developed primarily close to the
14 supports where diagonal tension failure occurred, as discussed in the previous section. Diagrams for
15 the three strengthened specimens lie in-between those for the unstrengthened ones, as far as maximum
16 elongation is concerned, but clearly closer to that of SVM, which was anticipated since these
17 specimens were also flexure-dominated. Among the strengthened specimens, elongation of the strips
18 was higher for the specimens (SS3X2M, SS12XM) strengthened with SPR than for the specimen
19 (SCM) strengthened with CFRP.

20 From the recorded force vs. horizontal elongation diagrams at the tension side of the right third of
21 the beam's length (HR), Fig. 11, it is seen that elongation of this region is very small in the case of
22 specimen SVM; in fact no elongation was recorded subsequent to the formation of the major flexural
23 crack at midspan, where all deformation concentrated. The elongation was larger in specimen SVS but
24 ceased after the formation of the diagonal tension crack. For the strengthened specimens the
25 elongation of the tension side increased at the end regions, apparently due to the fact that cracking in
26 these regions was much more pronounced than in the unstrengthened specimens (see Fig. 8); the
27 largest value was recorded for the SRP-strengthened specimen SS3X2M.

28 Referring now to the compression (upper) side of the beams, from the diagrams of Fig. 12
29 (recorded from LVDT 'HMC' in Fig. 7) it is seen that the only specimen wherein a typical flexural
30 behavior was observed (i.e. continuous shortening of the top side with increasing imposed deflection)
31 was specimen SVM. In all other specimens subsequent to the application of the maximum loading,
32 'unloading' occurred in the compression zone (i.e. reduced shortening with increasing imposed
33 vertical deflection), indicating a different inelastic deformation pattern. In the case of the strengthened
34 beams, it was observed that in the post-peak range (after debonding of the strips started) an elongation
35 of almost the entire specimen (including most of its top part) took place due to crack opening, which
36 resulted in recovering a rather substantial part (up to about 50%) of the shortening developed
37 previously in the upper part; recall that LVDT 'HMC' does not measure the deformation of the top

1 fiber, but that at a location a short distance (about 30 mm) from it, as shown in Fig. 7. This reduction
 2 in the compression strain can also be explained by the smaller neutral axis depth required to balance
 3 the reduced tensile force offered by steel reinforcement alone, compared to the stage prior to failure of
 4 the strip.

5 Finally, from the recorded force vs. diagonal elongation diagrams at the outer third of the beam's
 6 length (DL) shown in Fig. 13, it is clear that the only specimen that developed significant shear
 7 (diagonal tension) deformation was the shear-dominated SVS. In the flexure-dominated specimen
 8 SVM shear deformation was negligible, and in the three strengthened specimens it was very small and
 9 tended to stabilize, or even reduce, in the post-peak range. The diagrams in Fig. 13 confirm previous
 10 remarks that all reinforced polymer-strengthened beams were flexure-dominated.

11 Analytical Estimation of the Specimen Strength

12 The measurements obtained during the tests were used to estimate analytically the flexural and shear
 13 strength of both the initial (unstrengthened) and the strengthened beams, as reported in the following.

14 *Flexural Strength Estimation based on Measurements and First Principles*

15 On the basis of the discussions presented in the previous sections, it is clear that in all strengthened
 16 specimens, while the elongation of the reinforced polymer strips was significantly lower than the limit
 17 strain $\varepsilon_{f, \text{lim}}$ the strip was detached from the concrete surface; this detachment initiated at a flexural
 18 crack at mid-span.

19 For this well-known failure mechanism, the bending moment M_R resisted by the beam, can be
 20 estimated from the following relationship (Triantafillou 2003):

$$21 \quad M_R = A_{s1} \cdot f_y \cdot (d - \delta_G \cdot x) + A_f \cdot E_f \cdot \varepsilon_f \cdot (h - \delta_G \cdot x) + A_{s2} \cdot E_s \cdot \varepsilon_{s2} \cdot (\delta_G \cdot x - d_2) \quad (1)$$

22 where A_{s1} = area of tension reinforcement

23 A_{s2} = area of compression reinforcement

24 A_f = area of the reinforced polymer strip section

25 f_y = yield stress of steel reinforcement

26 E_f = modulus of elasticity of the reinforced polymer (parallel to the direction of the fibers)

27 E_s = modulus of elasticity of steel reinforcement

28 ε_f = strain of the reinforced polymer strip

29 ε_{s2} = strain of compression steel reinforcement

30 d = distance between the center of tension reinforcement and the top fiber of the section
 31 (effective depth)

32 h = height of specimen section

33 d_2 = distance between the center of compression reinforcement and the top fiber of the section

34 x = depth of the compression zone of the section

1 and

2 δ_G = height coefficient for the resultant of the internal compressive forces

$$3$$

$$4 \quad \delta_G = \begin{cases} \frac{8 - 1000 \cdot \varepsilon_c}{4 \cdot (6 - 1000 \cdot \varepsilon_c)} & \text{for } \varepsilon_c \leq 0.002 \\ \frac{1000 \cdot \varepsilon_c \cdot (3000 \cdot \varepsilon_c - 4) + 2}{2000 \cdot \varepsilon_c \cdot (3000 \cdot \varepsilon_c - 2)} & \text{for } 0.002 \leq \varepsilon_c \leq 0.0035 \end{cases} \quad (2)$$

5

6 The strain (ε_c) at the compressed part of the section of the specimens is estimated from the measured
 7 shortening (LVDT 'HMC'), while the strain (ε_f) of the reinforced polymer strip is estimated from the
 8 measured elongation (LVDT 'HMT'). Using the measured values of ε_c and ε_f into equations (2) and
 9 Bernoulli's principle, the coefficient δ_G and the depth of the compression zone of the section x can be
 10 found. The flexural capacity of the specimens can then be estimated from equation (1). From the
 11 moment capacity, the maximum shear in the specimens can be found from equilibrium.

12 The bending moment carried by the reinforced polymers ($M_{R,f}$) is given by the second term of
 13 equation (1) and the corresponding shear ($V_{R,f}$) resisted by the SRP or CFRP strips can be found from
 14 equilibrium.

15 It is known from the literature (e.g. Teng et al. 2002), that in regions of beams where flexural
 16 cracking exists the effective strain (ε_f) of the reinforced polymer, and hence the force that causes
 17 debonding, are increased. This increase was estimated for the beams of the present study by taking the
 18 average value of $(V_{deb,exp} - V_{crit,SVM})/V_{R,f}$, where $V_{deb,exp}$ is the shear at debonding (estimated from
 19 measured values) and $V_{crit,SVM}$ is the shear carried by the reference specimen SVM at yielding of the
 20 flexural reinforcement. The average value of this ratio was found to be 1.40, which is higher than the
 21 value 1.30 suggested by Teng et al. (2002), hence the maximum shear (corresponding to debonding)
 22 for the strengthened beams was subsequently estimated from

$$23 \quad V_{deb} = V_{crit,SVM} + 1.40 \cdot V_{R,f} \quad (3)$$

24 and $V_{deb} = P_{deb}/2$ where P_{deb} the load applied at the time of debonding (see Fig. 14). For the estimation
 25 of the effective elongation of the strips, just prior to detachment, the constant moment in the middle
 26 third of the length of the specimen was used. Results from the equations given in this section, along
 27 with the pertinent experimental measurements, are reported in Table 2.

28 Table 3 summarizes the analytically calculated strengths of the strengthened specimens, according
 29 to ACI 440R-08, and the Greek Code for Interventions (which is compatible with Eurocode 8 – Part
 30 3), as well as the corresponding measured strengths. Predictions of the Greek version of EC8-3 are
 31 quite close to the test results, while those from ACI 440 provide conservative estimates (up to 13%
 32 lower than the measured values). The reason for the latter conservatism was found to be eqn. 10-2 of
 33 ACI 440, which gives much lower effective strain values for the FRP than its 2002 edition, especially

1 for low concrete strengths, as was the case here. It is worth noting that the strengths found using the
2 2002 edition varied from 95% to 101% the measured values.

3 *Shear strength estimation for specimen SVS by the use of measurements*

4 Among the tested specimen reported herein, only SVS was shear-dominated, hence an attempt to
5 predict its shear strength using existing relationships in combination with measured test quantities was
6 made. Most of current codes (but not Eurocode 2) specify that the shear strength V_R can be determined
7 as the sum of the ‘concrete contribution’ V_c and the contribution of shear reinforcement (through the
8 truss mechanism) V_w . Introducing the measured stress of the stirrups in the equation for V_w and adding
9 the concrete contribution from the Prestandard version of Eurocode 2 (which is also adopted in the
10 Greek Concrete Code), the estimated shear strength of beam SVS was found to be 136.85 kN, which
11 corresponds to an applied load of 273.7 kN; as shown in Table 2, this is very close to the value
12 measured during the test (263.6 kN).

13

14 **Relative Efficiency of Strengthening Techniques**

15 Given the fact that SRP is generally less expensive than CFRP, it is important for practical application
16 to have some quantitative information regarding the relative efficiency of each composite material in
17 strengthening the specimens of the present study. Table 4 shows the strength increase (ratio of
18 measured ultimate load of strengthened specimen to that of the unstrengthened specimen SVM), and
19 the ratio of deflection at midspan corresponding to the maximum measured load (P_{max}) to that of the
20 CFRP- strengthened specimen SCM; the latter provides a relative measure of the deformability of the
21 strengthened members. It is seen that as far as strength is concerned all three composite strips had a
22 similar efficiency, i.e. increases in strength varied between 86% and 92%. The ratio $E_f A_f$ of SRP to
23 CFRP strips used for strengthening the beams was very close to unity, hence the percentage increases
24 are directly comparable; it should also be recalled that strength of these specimens was controlled by
25 the debonding failure mode. It is noted here that although strength increases up to 160% are possible,
26 much lower percentages are advisable for practical design (ACI 2008) due to additional requirements
27 such as ductility, serviceability, and possible failure of the FRP system due to damage or vandalism.

28 Unlike strength, differences in deformability are more noticeable between CFRP and SRP
29 strengthening, the latter leading to deflections up to 17% higher than that of the CFRP-strengthened
30 beam. Among the two types of SRP used, that with a large number of twisted wires (12X) was clearly
31 more efficient with respect to deformability, but slightly less efficient with respect to strength increase.
32 Finally, comparison of the axial deformation of the reinforced polymer strip corresponding to the
33 maximum load has shown that in specimens SS3X2M and SS12XM, this was 15% and 50% higher,
34 respectively, than that of the CFRP- strengthened specimen, which indicates an increased axial
35 flexibility of the SRP-strengthened members. The amount of energy dissipated by each specimen that

1 failed in a flexural way is given in figure 15. It is clear that, among the considered specimens,
2 SRP12X dissipated the highest amount of energy. By considering also the highest deformation
3 capacity that SRP12X developed, this material seems to be more suitable for strengthening of
4 reinforced concrete beams than SRP3X2.

5 **Conclusions**

6 From the first part of the study, involving tension tests of reinforced polymer materials, it was
7 confirmed that the stress – strain curves of SRP strips have a small inelastic branch prior to fracture, in
8 contrast with CFRP for which the stress – strain curve is linear up to fracture. On the other hand,
9 fracture strain had similar values for both materials.

10 Bond tests showed that the CFRP strips had higher debonding strength than SRP strips, which is in
11 line with previous findings that bond strength of strips is proportional to the square root of their
12 modulus of elasticity. The width of the strip was found to affect the bond strength between the
13 reinforced polymer and the concrete; however, the increase in bond strength was not directly
14 proportional to the width of the reinforced polymer. The two different anchorage lengths used for the
15 tested strips (300 mm and 150 mm), were not found to have any noticeable effect on the debonding
16 strength. This is not surprising if one notes that the effective anchorage length for the tested strips was
17 lower than 150 mm. From the analytical models used for predicting the experimentally measured bond
18 strengths, the model proposed by Chen and Teng (2001) was found to better match the test values.

19 The main part of the study, involving testing of full-scale beam specimens, showed that proper use
20 of SRP strips as externally-bonded tensile reinforcement can increase the flexural strength up to 92%,
21 which is substantially higher than that required in practice; it is recalled here that current codes place
22 limits on the amount of strengthening, so that in the event that the reinforced polymer system is
23 damaged (e.g. due to damage or vandalism), the structure will still be capable of resisting a reasonable
24 level of load without collapse (ACI 2008). These materials can be deemed equally effective as CFRPs
25 in increasing the flexural strength of R/C beams. After debonding of the strips, the strength of the
26 specimens was found to be slightly lower than the strength of the corresponding unstrengthened
27 specimen; this was attributed to the different cracking pattern, due to which the steel bars did not
28 develop (at that stage) their full strength as in the unstrengthened beam. Higher deformation capacity
29 (up to 17%) was found for the specimens strengthened with SRP, compared to the specimen
30 strengthened with CFRP. Providing additional anchorage length (600 mm beyond the support) to the
31 strips of the SRP and CFRP strengthened specimens, was not found to lead to increased strength or
32 deformation capacity, with respect to that of the specimen where the strip was anchored close to the
33 support in an area subjected to tension. As expected, all strengthened specimens failed by debonding
34 of the strip; debonding initiated close to a flexural crack at mid-span.

35 From the analytical part of the study, the most interesting finding was that the increase in the
36 effective strain (hence the strength) of reinforced polymer-strengthened beams attributed to the

1 presence of flexural cracks was 40%, which is slightly higher than the value reported in previous
2 studies (Teng et al. 2002); of course this 40% cannot be claimed to be a value of general validity.

3 Finally, comparisons of analytically predicted strengths with experimentally measured values has
4 shown that the equations developed for FRP-strengthened beams can also be used for SRP-
5 strengthened members.

6 **Acknowledgements**

7 The research project, results of which are present in this paper, was jointly funded by EU-European
8 Social Fund, the Greek Ministry of Development-GSRT, and Sika – Hellas.

9 **References**

10 American Concrete Institute ACI (2008), “Guide for the Design and Construction of Externally
11 Bonded FRP Systems for Strengthening Concrete Structures”, ACI 440.2R-08, Farmington Hills,
12 Michigan.

13 Barton, B.L., Wobbe, E., Dharani, L.R., Silva, P.F., Birman V., Nanni, A., Alkhrdaji, T., Thomas, J.
14 and Tunis, T. (2005) “Characterization of RC Beams Strengthened by Steel Reinforced Polymer and
15 Grout (SRP and SRG) Composites”, Materials Science and Engineering A, Vol. 412, p. 129.

16 Cancelli, A., Aiello, M., and Casadei, P. (2007) “Experimental Investigation on Bond Properties of
17 SRP/SRG – Masonry Systems”, 8th Int. Symp. FRP Reinforcement for Concrete Structures, FRPRCS-
18 8, University of Patras, Greece, Paper 18-11, pp.10.

19 Casadei, P., Nanni, T., Alkhrdaji, T. and Thomas, J. (2005) “Performance of Double-T Prestressed
20 Concrete Beams Strengthened with Steel Reinforced Polymer”, Advances in Structural Engineering -
21 An International Journal, Vol. 8, No 4, pp. 427-442.

22 CEN (2005) “Eurocode 8: Design of Structures for Earthquake Resistance-Part 3: Assessment and
23 Retrofitting of Buildings”, (preEN 1998-3:200X), Brussels.

24 Chen, J., and Teng, J. (2001), “Anchorage Strength Models for FRP and Steel Plates Bonded to
25 Concrete”, Journal of Structural Engineering, Vol.127, No. 7, pp. 784-791.

26 Figeys, W., Schueremans, L., Brosens, K. and Van Gemert, D. (2005) “Strengthening of Concrete
27 Structures using Steel Wire Reinforcement Polymer”, 7th Int. Symp. FRP Reinforcement for Concrete
28 Structures, SP-230, ACI Vol. 1, Farmington Hills, USA, Paper # 43, pp. 743-762.

29 Huang, X., Birman, V., Nanni, A. and Tunis, G. (2005) “Properties and Potential for Application of
30 Steel Reinforced Polymer (SRP) and Steel Reinforced Grout (SRG) Composites”, Composites, Part
31 B, Vol. 36, No 1, pp. 73-82.

- 1 Kim, J.Y., Fam, A., Kong, A. and El-Hacha, R. (2005) "Flexural Strengthening of RC Beams Using
2 Steel Reinforced Polymer (SRP) Composites", 7th Int. Symp. FRP Reinforcement for Concrete
3 Structures, SP-230, ACI Vol. 1, Farmington Hills, USA, Paper # 93, pp. 1647-1664.
- 4 Lopez, A., Galati, N., Alkhrdaji, T. and Nanni, A. (2007) "Strengthening of a Reinforced Concrete
5 Bridge with Externally Bonded Steel Reinforced Polymer (SRP)", *Composites Part B*, Vol. 38, No 4,
6 pp. 429-436.
- 7 Matana, M., Nanni, A., Dharani, L., Silva, P. and Tunis, G. (2005) "Bond Performance of Steel
8 Reinforced Polymer and Steel Reinforced Grout", *Proceedings of International Symposium on Bond
9 Behaviour of FRP in Structures, BBFS 2005*, Paper # 101.
- 10 Mitolidis, G., Salonikios, T. and Kappos, A. (2008a) "Bond Tests of SRP and CFRP – Strengthened
11 Concrete Prisms", 4th Int. Conference on FRP Composites in Civil Engineering (CICE2008), 22-24
12 July, Zurich, Switzerland, Paper # E111, (7.C.5)
- 13 Mitolidis, G.J., Salonikios, T.N., and Kappos, A.J. (2008b) "Mechanical and Bond Characteristics of
14 SRP and CFRP Reinforcement – A Comparative Research", *The Open Construction and Building
15 Technology Journal*, 2, pp. 207-216.
- 16 Prota, A., Manfredi, G., Nanni, A., Cosenza, E. and Pecce, M. (2004) "Flexural Strengthening of RC
17 Beams using Emerging Materials: Ultimate Behavior", 2nd Int. Conf. on FRP Composites in Civil
18 Engineering, CICE 2004, Adelaide, Australia, pp. 163-170.
- 19 Saber, N., Hassan, T., Abdel-Fayad, A. S. and Gith, H. (2008) "Flexural behavior of concrete beams
20 strengthened with steel reinforced polymers", 4th Int. Conf. on FRP Composites in Civil Engineering,
21 CICE 2008, Zurich, Switzerland, 6 pp.
- 22 Teng, J.G., Chen, J.F., Smith, S.T. and Lam, L. (2002) "FRP Strengthened RC Structures", John
23 Wiley & Sons Ltd, Chichester, England, 245pp.
- 24 Toutanji, H., Saxena, P., Zao, L. and Ooi, T. (2007) "Prediction of Interfacial Bond Failure of FRP-
25 Concrete Surface", *Journal of Composites for Construction*, ASCE, Vol.11, No. 4, pp.427-436.
- 26 Triantafillou, T. (2003) "Strengthening of R/C structures by the use of composite materials", 1st
27 Edition, Patras (in Greek).
- 28 Wobbe, E., Silva, P.F., Barton, B.L., Dharani, L.R., Birman, V., Nanni, A., Alkhrdaji, T., Thomas, J.
29 and Tunis, T. (2004) "Flexural Capacity of RC Beams Externally Bonded with SRP and SRG",
30 *Proceedings of Society for the Advancement of Material and Process Engineering, Symposium*, Long
31 Beach, Ca, USA.

1 **Table Captions**

2 Table 1. Specimen data and results from bond tests

3 Table 2. Comparison between calculated and measured strength (ultimate load) for the tested beams

4 Table 3. Comparison of the measured experimental strength with predictions according to ACI-440R-
5 08 and EC8-3 and Greek Code for Interventions

6 Table 4. Ratios of measured strengths (ultimate loads) and deflections of strengthened beams to that of
7 the reference specimen (SVM)

8

9 **Figure Captions**

10 Fig. 1. Tensile stress-strain diagrams for unidirectional CFRP and SRP strips, and for steel
11 reinforcement.

12 Fig. 2. Bond tests of 50 mm × 150 mm SRP and CFRP strips: (a) Test set-up; (b) Load vs. slip
13 diagrams (detachment force is equal to $0.5P_{tot}$).

14 Fig. 3 Comparisons of measured values of bond strength with those predicted using the models of (a)
15 Chen & Teng, 2001; (b) Yang et. al, 2001.

16 Fig. 4. Details of the beam specimens

17 Fig. 5. Support details of the specimens.

18 Fig. 6. Experimental set-up

19 Fig. 7. LVDT arrangement on the specimen

20 Fig. 8. Failure modes of specimens; (a) SVM, (b) SVS, (c) SS3X2M, (d) SS12XM and (e) SCM.

21 Fig. 9. Load vs. mid-span displacement (LVDT 'MD', see Fig. 7) curves for the specimens

22 Fig. 10. Load vs. horizontal elongation at mid-span (LVDT 'HMT') curves

23 Fig. 11. Load vs. horizontal elongation curves on the left third (LVDT 'HL') of the span.

24 Fig. 12. Load vs. mid-span horizontal compression (LVDT 'HMC') curves

25 Fig. 13. Load vs. diagonal elongation (LVDT 'DL') curves

26 Fig. 14. Schematic load vs. deflection curve, indicating characteristic load values

27 Fig. 15. Comparative diagram of the absorbed energy for the specimens with flexural failure (the same
28 deformation level was considered for all specimens).

1 Table 1. Specimen data and results from bond tests

2

| Specimen | Concrete Grade | $t_f \times b_f \times L$ | Type of Strip | $0.5P_{tot}$ | $s_{tot}^*/s_{tot,u}$ | $\frac{\sqrt{E_i}}{\sqrt{E_{SRP12X}}} \cdot \frac{P_{SRP12X}}{P_i}$ |
|---------------|----------------|---------------------------|---------------|--------------|-----------------------|---|
| | | mm | | kN | mm | |
| CFRP-5X15NS | C20/25 | 1.20×50×150 | CFRP | 19.0 | 0.38/0.52 | 1.13 |
| CFRP-5X30NS | C20/25 | 1.20×50×300 | CFRP | 18.5 | 0.50/0.70 | 1.16 |
| SRP12-5X15NS | C20/25 | 1.23×50×150 | SRP12X | 13.7 | 1.09/1.25 | 1.01 |
| SRP12-5X30NS | C20/25 | 1.23×50×300 | SRP12X | 13.5 | 0.55/1.11 | 1.02 |
| SRP12-8X15NS | C20/25 | 1.23×80×150 | SRP12X | 19.0 | 0.55/ – | 1.05 |
| SRP12-8X30NS | C20/25 | 1.23×80×300 | SRP12X | 21.0 | 0.58/0.99 | 0.95 |
| SRP3X2-5X15NS | C20/25 | 1.23×50×150 | SRP3X2 | 15.0 | 0.45/0.56 | 0.99 |
| SRP3X2-5X30NS | C20/25 | 1.23×50×300 | SRP3X2 | 14.0 | – /0.60 | 1.07 |
| SRP3X2-8X15NS | C20/25 | 1.23×80×150 | SRP3X2 | 20.3 | 0.37/0.79 | 1.06 |
| SRP3X2-8X30NS | C20/25 | 1.23×80×300 | SRP3X2 | 22.0 | 1.29/1.28 | 0.97 |
| CFRP-5X15HS | C35/45 | 1.20×50×150 | CFRP | 18.7 | 0.21/0.25 | 1.14 |
| CFRP-5X30HS | C35/45 | 1.20×50×300 | CFRP | 18.8 | 0.23/0.60 | 1.14 |
| SRP12-5X15HS | C35/45 | 1.23×50×150 | SRP12X | 13.8 | 0.23/0.51 | 1.00 |
| SRP12-5X30HS | C35/45 | 1.23×50×300 | SRP12X | 14.5 | 0.51/1.29 | 0.96 |
| SRP3X2-5X15HS | C35/45 | 1.23×50×150 | SRP3X2 | 13.8 | – / 0.50 | 1.08 |
| SRP3X2-5X30HS | C35/45 | 1.23×50×300 | SRP3X2 | 15.3 | 0.28/0.54 | 0.98 |

* measured displacement between the outer points of the bonded lengths.

3

Table 2. Comparison between calculated and measured strength (ultimate load) for the tested beams

| Specimen | Calculated strength | | | | Measured Strength | | | | $\frac{P_{deb,calc}}{P_{u,meas}}$ - |
|---------------|---------------------|------------|-----------|-----------|-------------------|------------|-----------|-----------|--|
| | P_{deb} | P_{crit} | P_{fin} | P_u | P_{deb} | P_{crit} | P_{fin} | P_u | |
| | <i>kN</i> | <i>kN</i> | <i>kN</i> | <i>kN</i> | <i>kN</i> | <i>kN</i> | <i>kN</i> | <i>kN</i> | |
| <i>SVS</i> | - | - | - | 273.70 | - | - | - | 263.60 | 1.04 |
| <i>SVM</i> | - | - | 113.24 | - | - | - | 117.60 | - | 0.96 |
| <i>SS3X2M</i> | 231.01 | 95.56 | 113.24 | - | 225.60 | 104.40 | 108.40 | - | 1.02 |
| <i>SSI2XM</i> | 216.45 | 95.56 | 113.24 | - | 218.00 | 83.60 | 102.80 | - | 0.99 |
| <i>SCM</i> | 203.36 | 95.56 | 113.24 | - | 224.80 | 96.40 | 105.20 | - | 0.91 |

Note: P_{deb} , P_{crit} , and P_{fin} are defined in Fig. 14.

Table 3. Comparison of the measured experimental strength with predictions according to ACI-440R-02, and EC8-3 and Greek Code for Interventions

| Specimen | ACI 440R-08 | | | EC8-3 & Greek Code for Interventions | | | Measured Strength |
|---------------|-------------------|---------------|---------------------------------|--------------------------------------|---------------|---------------------------------|-------------------|
| | Flexural Strength | Ultimate Load | $\frac{P_{u,theor}}{P_{u,exp}}$ | Flexural Strength | Ultimate Load | $\frac{P_{u,theor}}{P_{u,exp}}$ | |
| | M_u | P_u | | M_u | P_u | | |
| | <i>kNm</i> | <i>kN</i> | – | <i>kNm</i> | <i>kN</i> | – | <i>kN</i> |
| <i>SS12XM</i> | 105.95 | 192.63 | 0.88 | 116.41 | 211.65 | 0.97 | 218.00 |
| <i>SS3X2M</i> | 109.37 | 198.85 | 0.88 | 121.36 | 220.65 | 0.98 | 225.60 |
| <i>SCM</i> | 107.58 | 195.60 | 0.87 | 119.97 | 218.13 | 0.97 | 224.80 |

Table 4. Ratios of measured strengths (ultimate loads) and deflections of strengthened beams to that of the reference specimen (SVM)

| SPECIMEN | P_{max} (<i>kN</i>) | P_{max} / P_{SVM} (%) | $\delta_{mid@Pmax}$ (<i>mm</i>) | $\delta_{mid@Pmax} /$ $\delta_{mid@Pmax,SCM}$ |
|----------------------|----------------------------|----------------------------|--------------------------------------|--|
| <i>SVM</i> | 117.6 | 100.0 | – | – |
| <i>SS3X2M</i> | 225.6 | 191.8 | 21.7 | 1.04 |
| <i>SS12XM</i> | 218.0 | 185.9 | 24.4 | 1.17 |
| <i>SCM</i> | 224.8 | 191.2 | 20.8 | 1.00 |

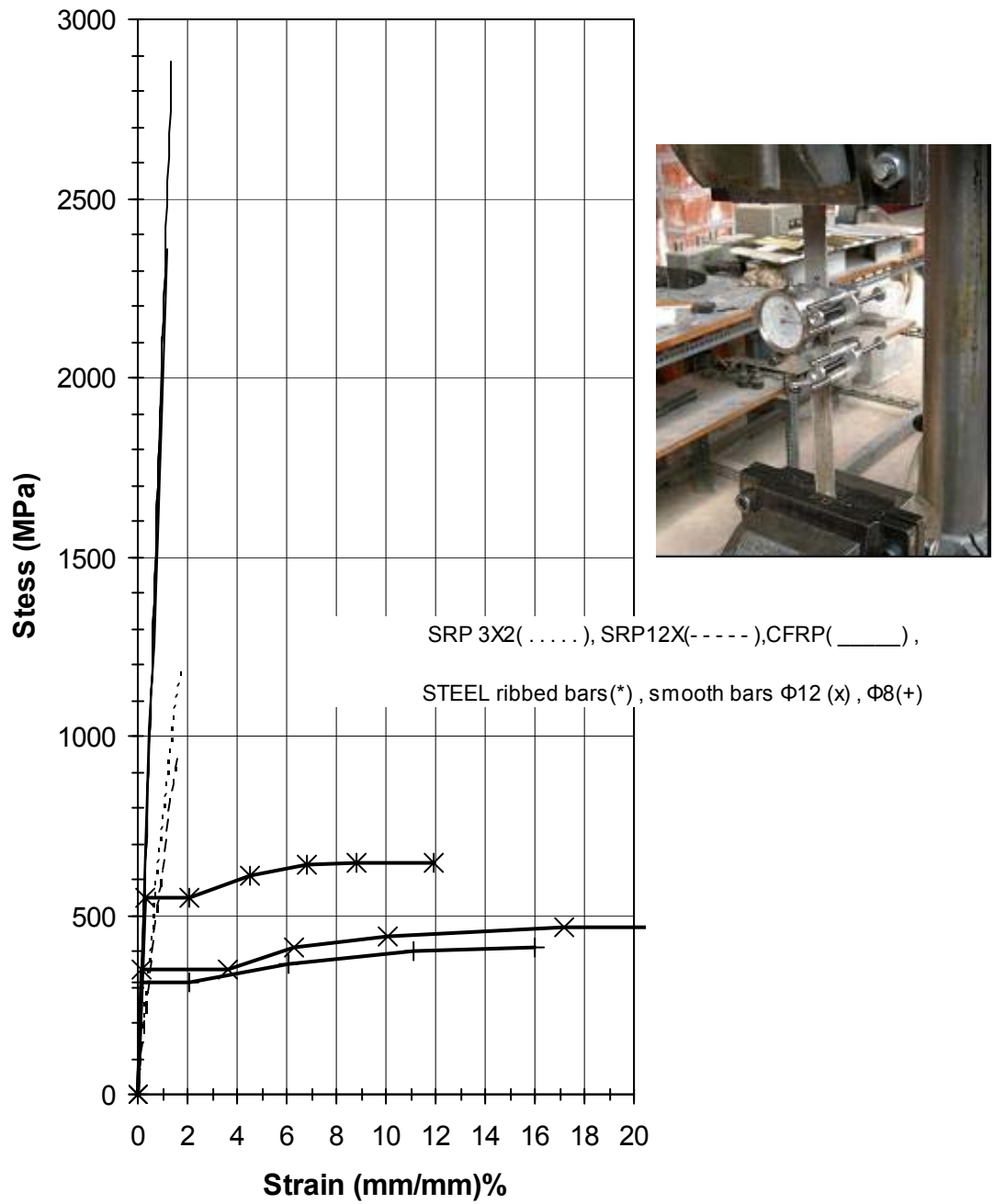
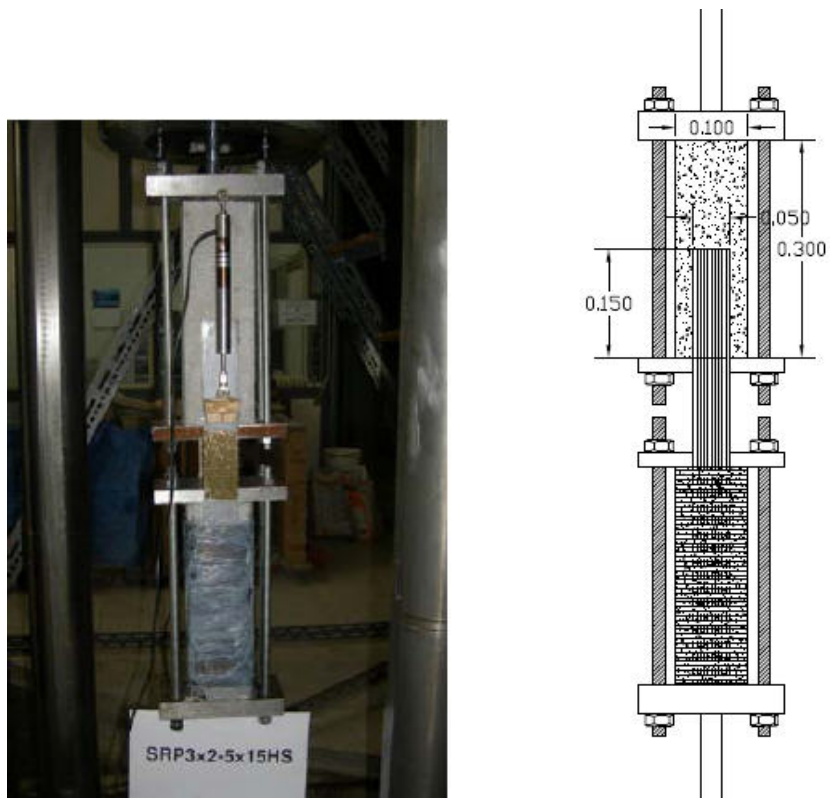
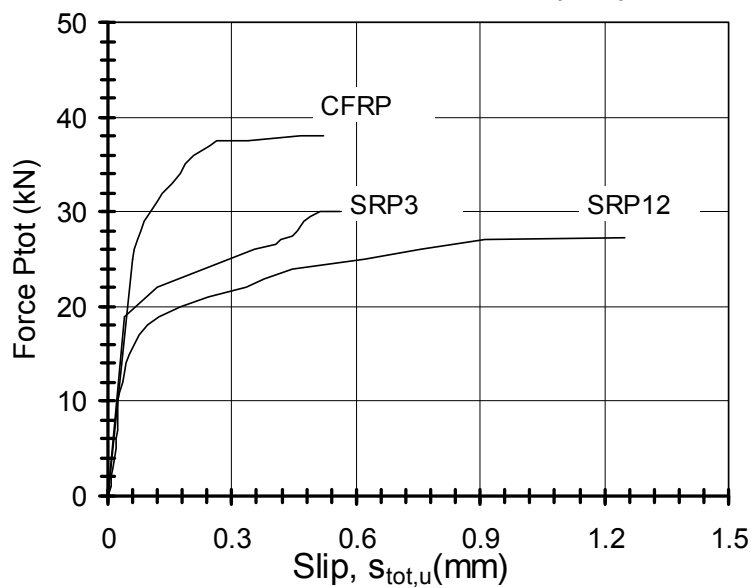


Fig. 1. Tensile stress-strain diagrams for unidirectional CFRP and SRP strips, and for steel reinforcement (the insert shows the test set-up).

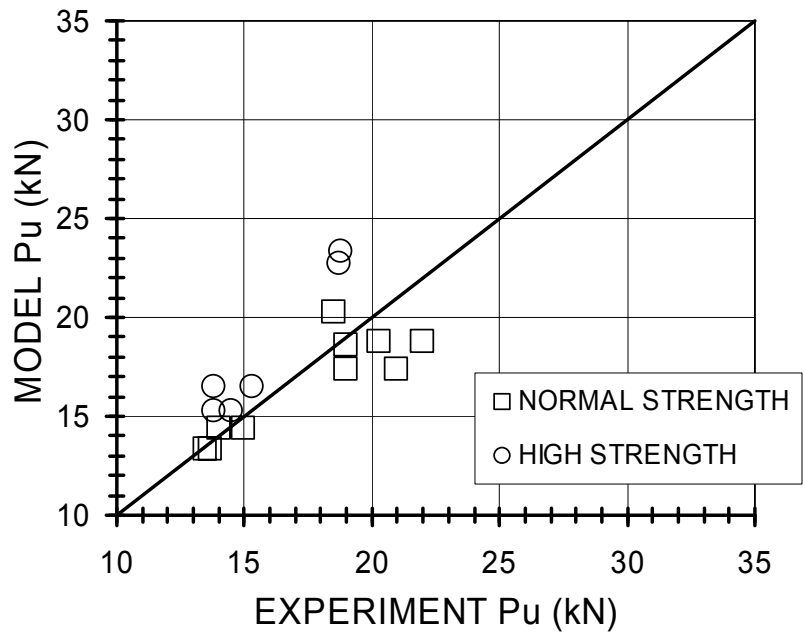


(a)

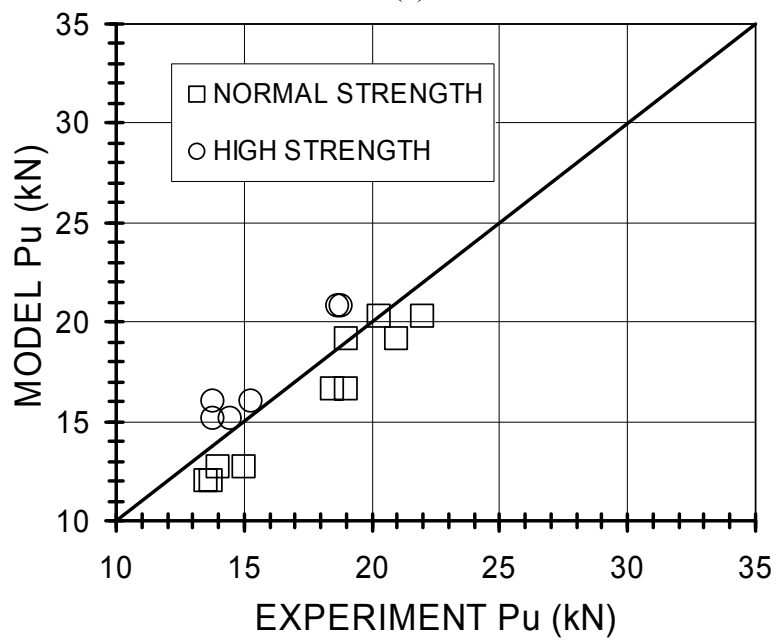


(b)

Fig. 2. Bond tests of 50 mm × 150 mm SRP and CFRP strips:
 (a) Test set-up; (b) Load vs. slip diagrams (detachment force is equal to $0.5P_{tot}$).



(a)



(b)

Fig. 3. Comparisons of measured values of bond strength with those predicted using the models of (a) Chen & Teng, 2001; (b) Yang et. al, 2001.

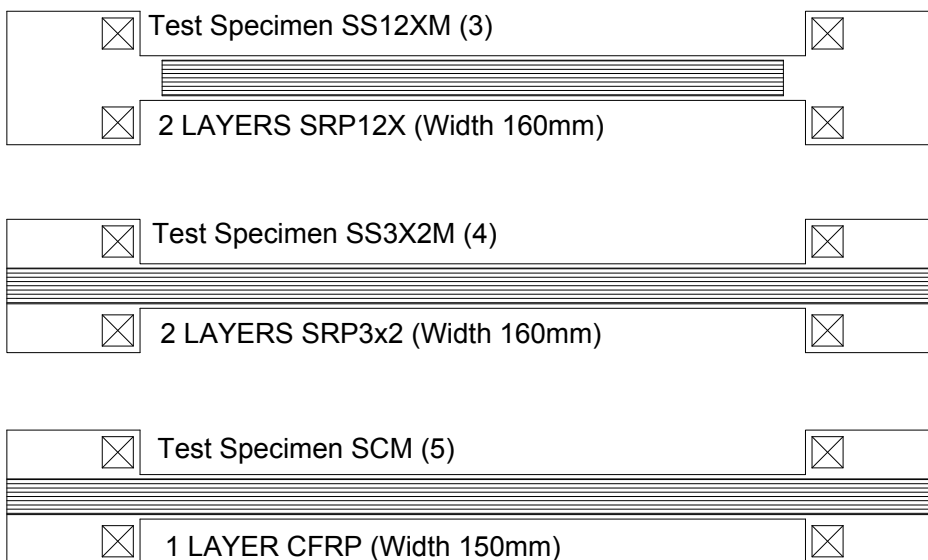
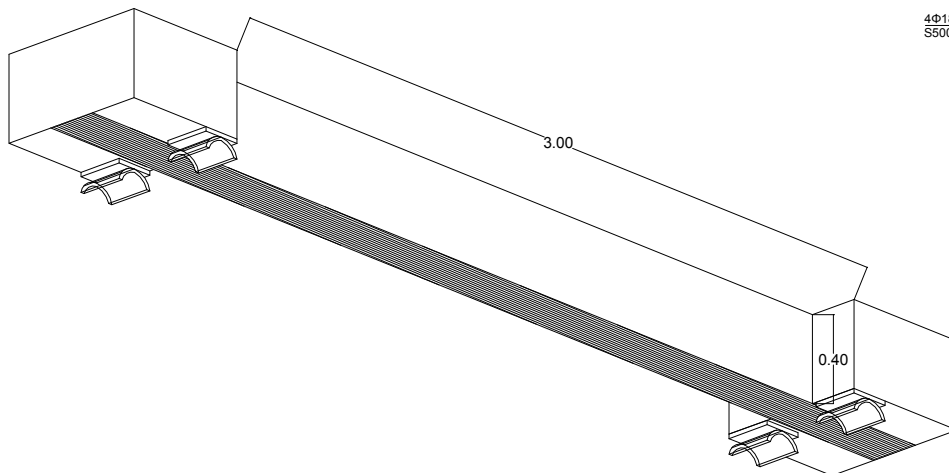
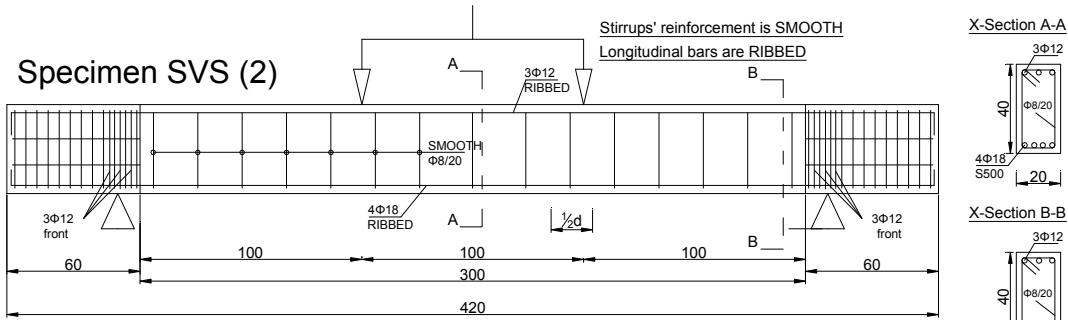
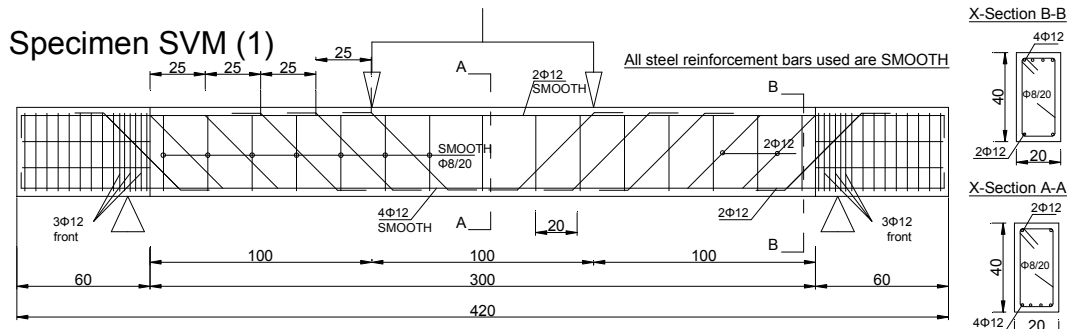


Fig. 4. Details of the beam specimens



Fig. 5. Support details of the specimens.

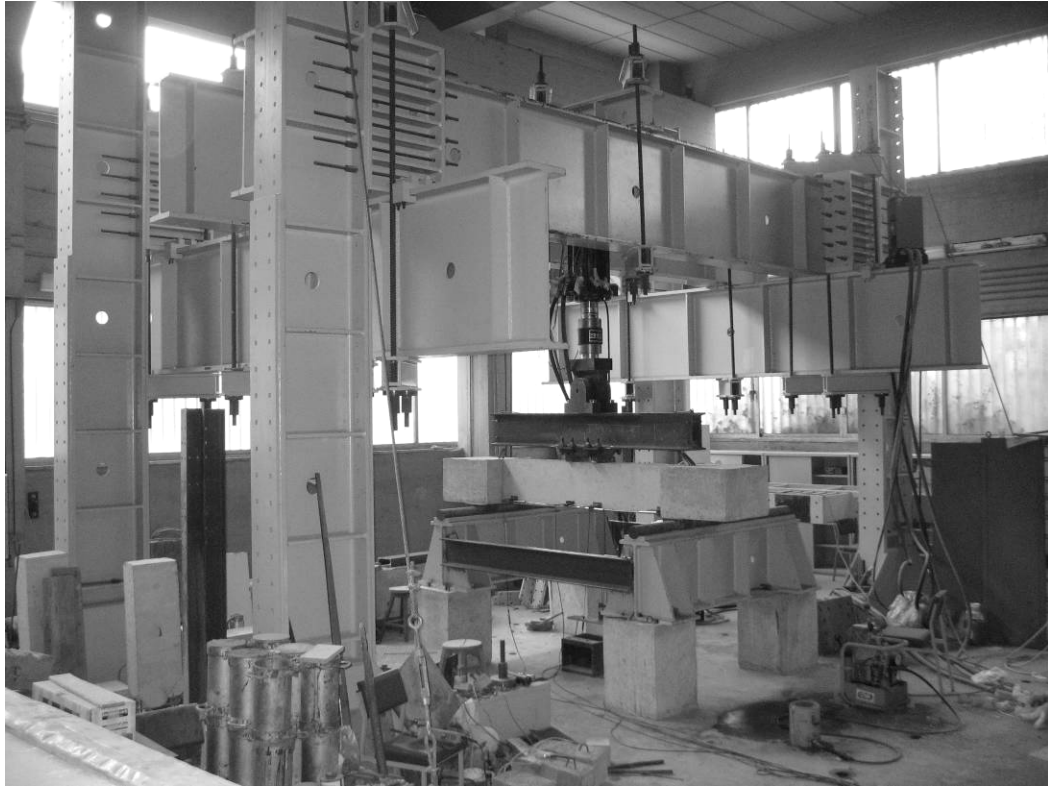


Fig. 6. Experimental set-up

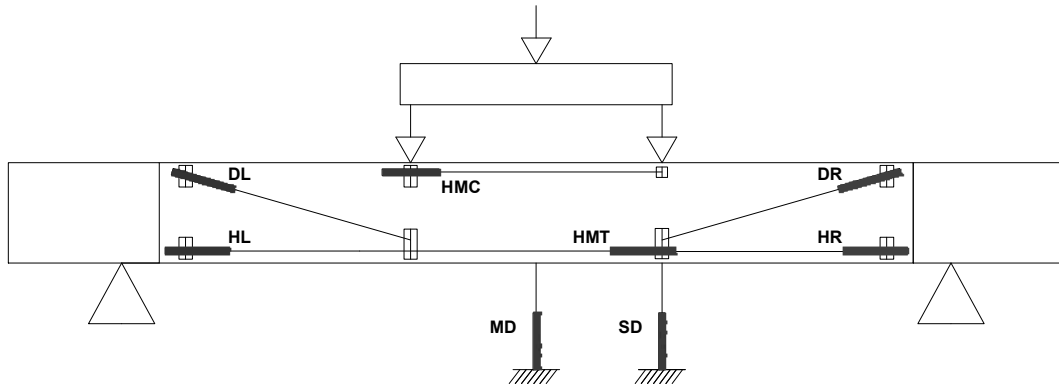
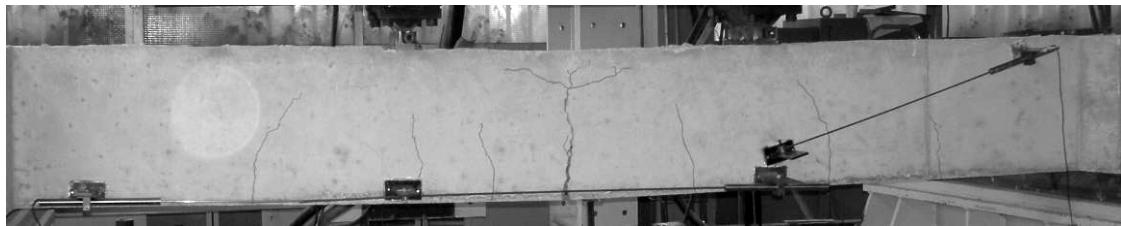


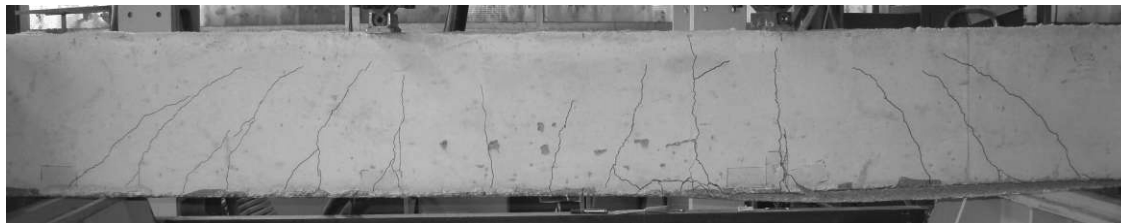
Fig. 7. LVDT arrangement on the specimen



(a)



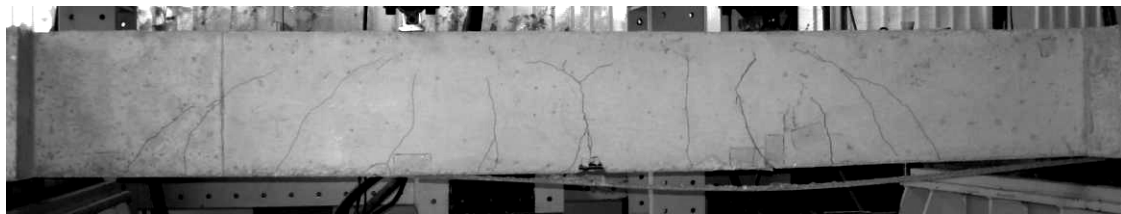
(b)



(c)



(d)



(e)

Fig. 8. Failure modes of specimens; (a) SVM, (b) SVS, (c) SS3X2M, (d) SS12XM and (e) SCM.

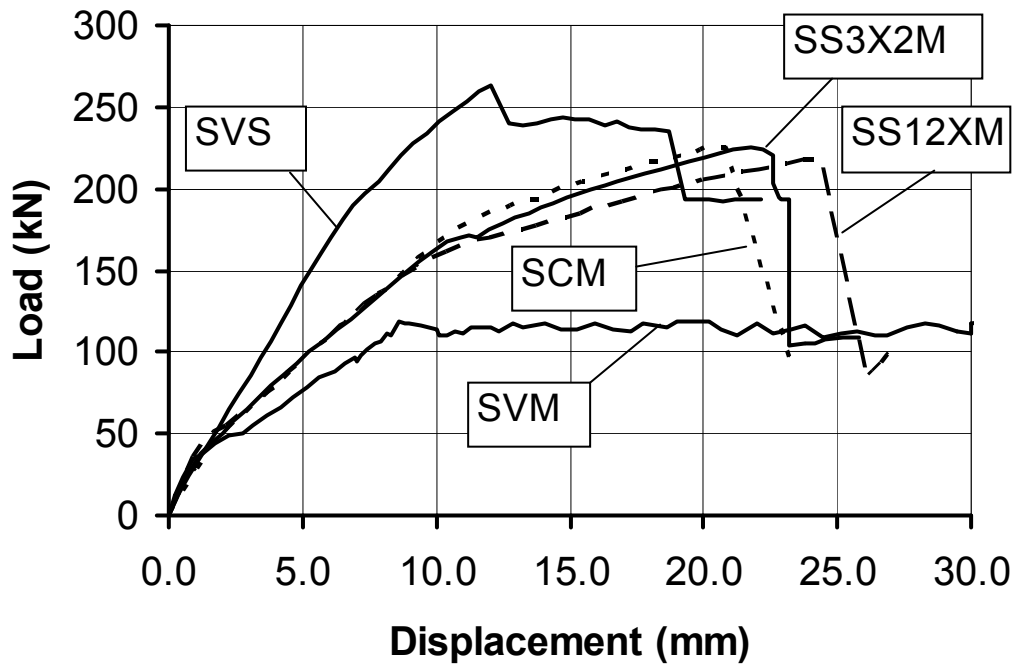


Fig. 9. Load vs. mid-span displacement (LVDT 'MD', see Fig. 7) curves for the specimens

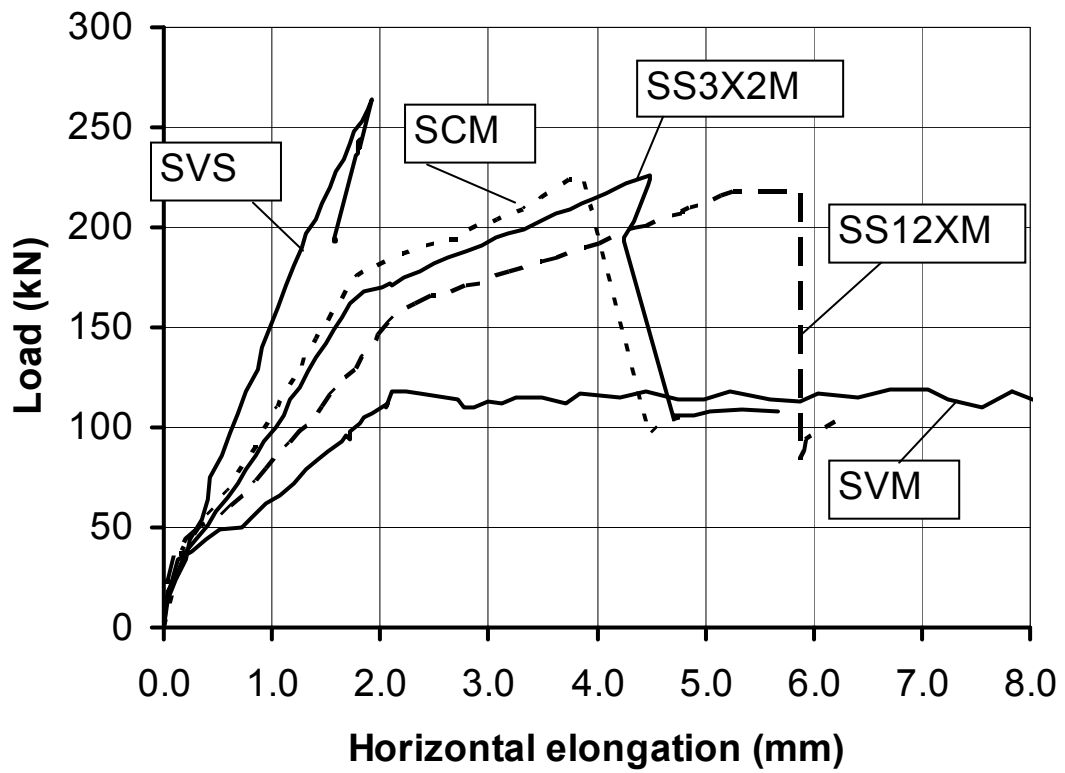


Fig. 10. Load vs. horizontal elongation at mid-span (LVDT 'HMT') curves

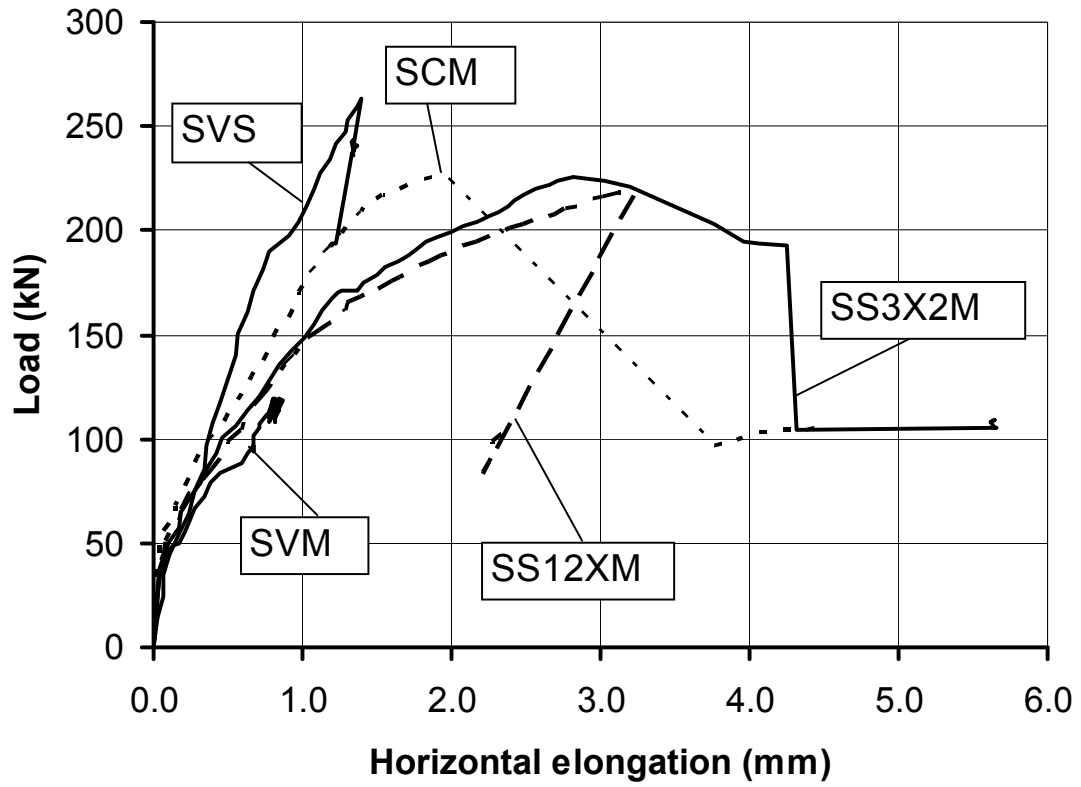


Fig. 11. Load vs. horizontal elongation curves on the left third (LVDT 'HL') of the span.

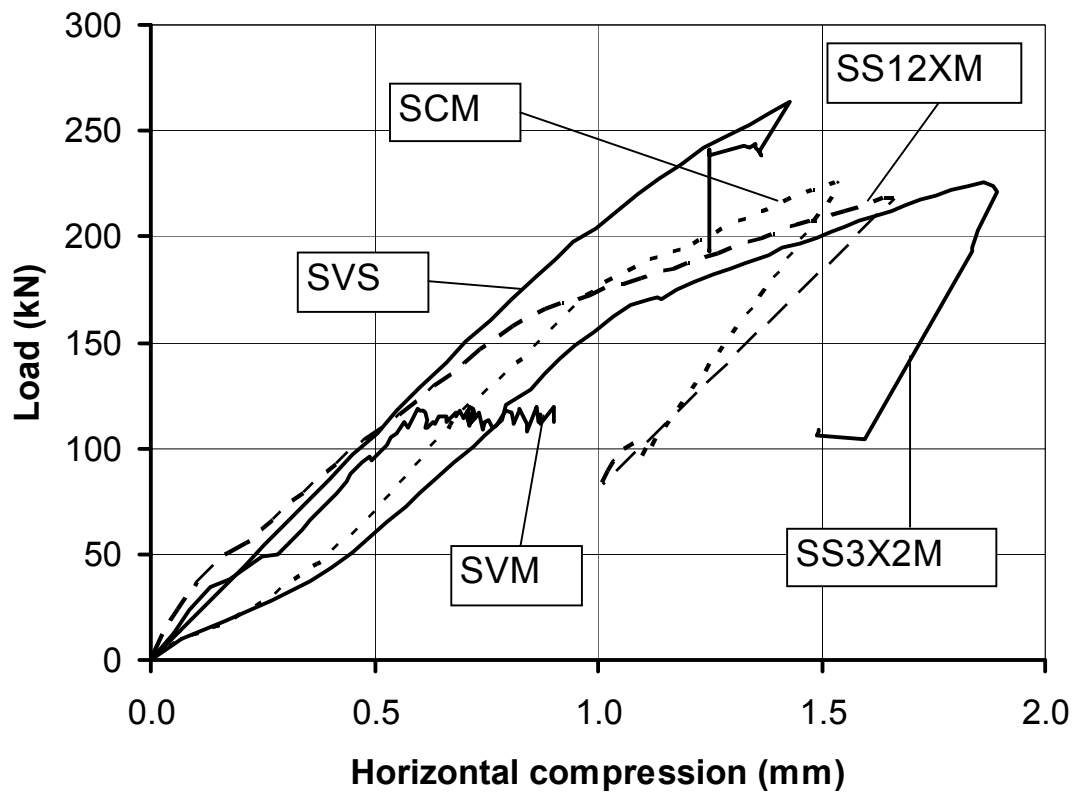


Fig. 12. Load vs. mid-span horizontal compression (LVDT 'HMC') curves

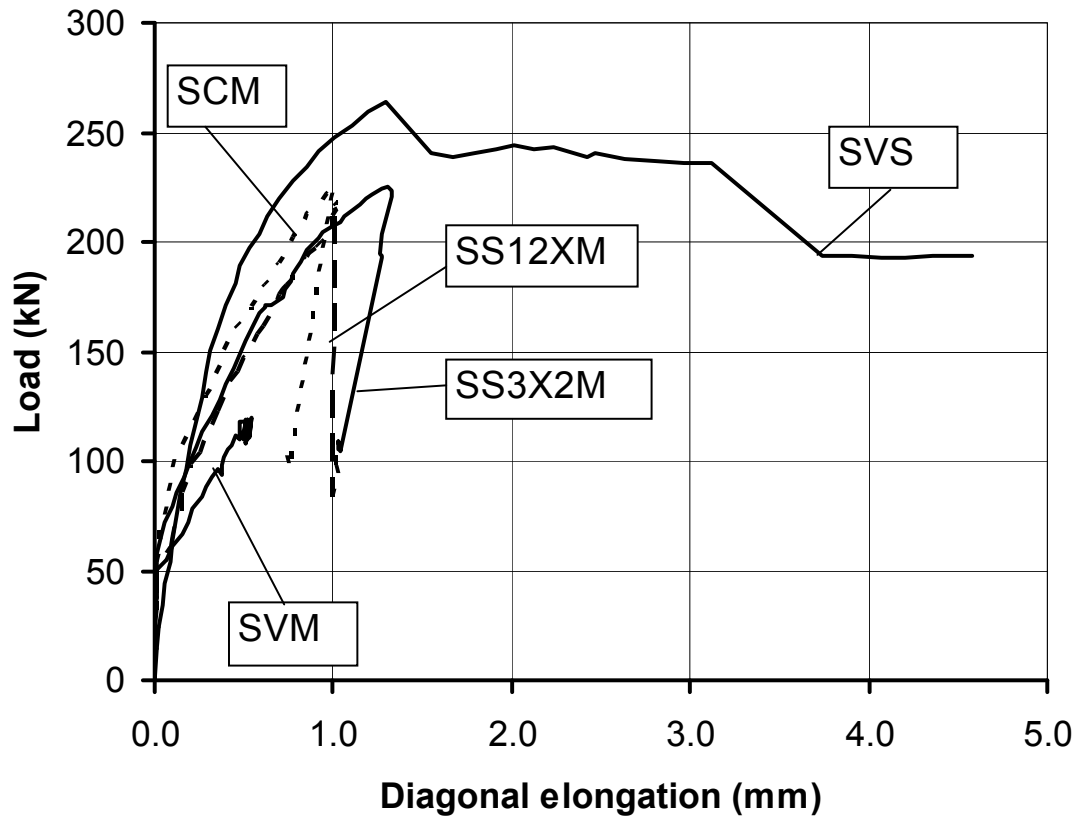


Fig. 13. Load vs. diagonal elongation (LVDT 'DL') curves

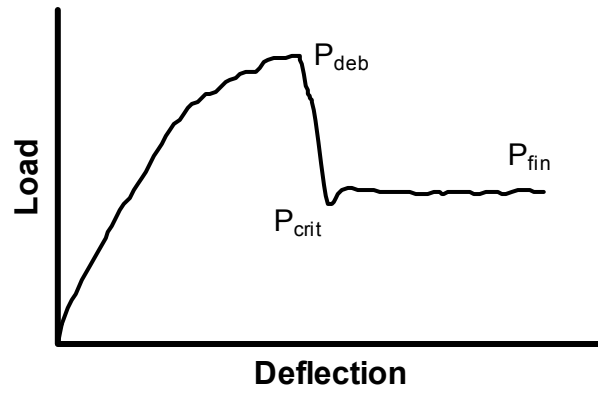


Fig. 14. Schematic load vs. deflection curve, indicating characteristic load (P) values

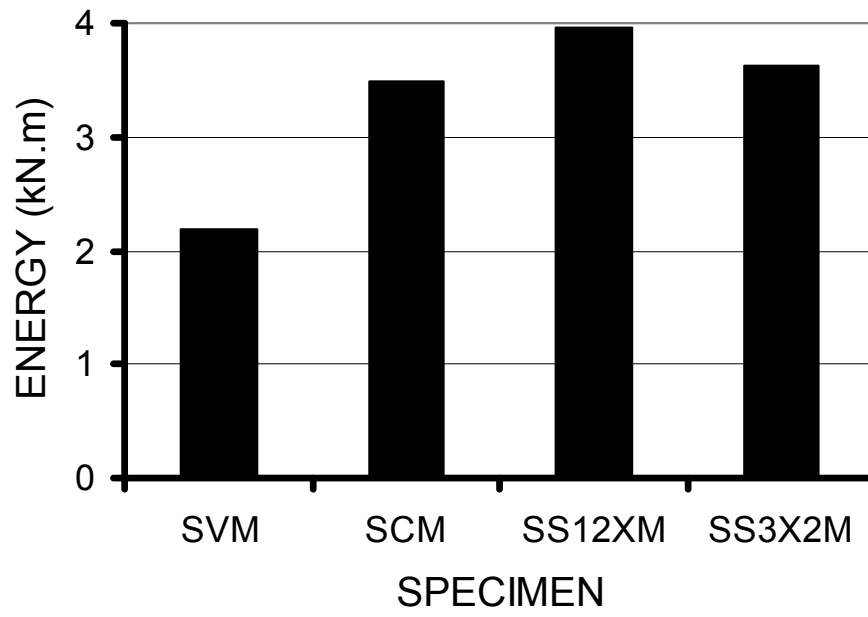


Fig. 15. Comparative diagram of the absorbed energy for the specimens with flexural failure (the same deformation level was considered for all specimens).